Lateral diffusion in an archipelago

Distance dependence of the diffusion coefficient

Michael J. Saxton

*Plant Growth Laboratory, University of California, Davis, California 95616; and Laboratory of Chemical Biodynamics, Lawrence Berkeley Laboratory, University of California, Berkeley, California 94720

ABSTRACT An understanding of the distance dependence of the lateral diffusion coefficient is useful in comparing the results of diffusion measurements made over different length scales, and in analyzing the kinetics of mobile redox carriers in organelles. A distance-dependent, concentration-dependent diffusion coefficient is defined, and it is evaluated by Monte Carlo calculations of a random walk by mobile point tracers in the presence of immobile obstacles on a triangular lattice, representing the diffusion of a lipid or a small protein in the presence of immobile membrane proteins. This work confirms and extends the milling crowd model of Eisinger, J., J. Flores, and W. P. Petersen (1986. Biophys J. 49:987–1001). Similar calculations for diffusion of mobile particles interacting by a hard-core repulsion yield the distance dependence of the self-diffusion coefficient. An expression for the range of short-range diffusion is obtained, and the distance scales for various diffusion measurements are summarized.

INTRODUCTION

Various cellular mechanisms have been shown to require lateral diffusion of membrane components (McCloskey and Poo, 1984; Peters, 1985; Edidin, 1987). The long-range lateral diffusion of mobile species in a cell membrane can be obstructed by the presence of immobile species, and the effect of these obstacles can be described by percolation theory. According to this theory (Stauffer, 1985; Feder, 1988), if the obstacles are immobile and randomly distributed, the long-range diffusion coefficient of the mobile species goes to zero when the area fraction c of obstacles is greater than the percolation threshold c_p.

At high concentrations of obstacles, long-range diffusion is blocked, but short-range diffusion is still possible. The question thus arises, when is diffusion long-range? Or, more generally, how does the lateral diffusion coefficient depend on the distance over which diffusion is measured? These questions arise in both experimental and physiological contexts.

In measurements of lateral diffusion by fluorescence photobleaching recovery, diffusion is measured over a distance comparable with the radius of the photobleached area (≈ 1 μm or more), whereas for excimer formation or other short-range interactions the distance is of the order of the average initial separation between reactants (typically 1–10 nm for excimer formation.) As Eisinger et al. (1986) have shown, the effect of obstacles is much different in these two cases.

Electron transfer in chloroplasts (Millner and Barber, 1984), endoplasmic reticulum (Gut et al., 1982), and mitochondria (Hackenbrock et al., 1986; Lenaz and Fato,

1986; Lenaz, 1988) is thought to require lateral diffusion of mobile redox carriers. The concentration of proteins in these membranes is high, so that long-range diffusion will be hindered. But if short-range diffusion is sufficient, a mobile-carrier mechanism is possible even above the percolation threshold.

Domains in cell membranes (Kleinfeld, 1987; Hui, 1987) may also influence lateral diffusion (Yechiel and Edidin, 1987; Cowan et al., 1987; Jacobson et al., 1987; Wolf, 1988). Domains may result from lateral phase separation in a lipid or lipid-protein mixture, or from protein segregation imposed by the cytoskeleton or other barriers. The treatment presented here applies to domains which exclude the diffusing species. A different treatment is required if the tracer can diffuse in both phases.

The topic of long-range versus short-range diffusion coefficients in lateral diffusion has been discussed qualitatively by several authors, including Galla et al. (1979), Kuo and Wade (1979), McCloskey and Poo (1984), Hackenbrock et al. (1986), Lenaz and Fato (1986), and Lenaz (1988). The question has been treated more quantitatively for two-dimensional diffusion by Eisinger et al. (1986), and for three-dimensional diffusion by Gaylor et al. (1979), among others (Pusey and Tough, 1985). Here we present a model of two-dimensional diffusion using Monte Carlo calculations and percolation theory. In the calculations, lattice sites are randomly obstructed; the obstructions are identified with immobile integral and peripheral proteins. A point tracer executes a random walk on the obstructed lattice, and the diffusion coeffi-

cient is obtained from the mean-square displacement $\langle r^2(t) \rangle$ of an ensemble of tracers. A preliminary version of this work was presented at the 1987 Biophysical Society meeting (Saxton, 1987a).

METHODS

Monte Carlo calculations were carried out for the diffusion of point tracers in the presence of mobile or immobile point obstacles on the triangular lattice as previously described (Saxton, 1987b). Obstacles are placed at random lattice points at the required concentration. A tracer is placed at a random unoccupied point and carries out a random walk, moving to unobstructed nearest-neighbor points. Values of $\langle r^2 \rangle$ are recorded periodically. For each initial distribution of obstacles, at least 100 tracers are used; for the shortest runs, 1,600 tracers are used. The calculation is repeated for 50–400 initial distributions of obstacles. A 256 × 256 triangular lattice is used, and periodic boundary conditions are imposed. The logarithmic correction described earlier (Saxton, 1987b) is not used, so that the distance-dependent diffusion coefficients include contributions from the long-time tail in $\langle r^2(t) \rangle$.

Several calculations are made for each concentration of obstacles, with different total times and time increments. Typically, D^* was calculated for 1–128 time steps with an increment of 1 step, 1–512 time steps with an increment of four steps, and so on to 32,768 time steps. For longer runs, much coarser intervals were used.

For clarity, duplicate points are omitted in the graphs. To show the statistical error, all data points for $c = 0.2$ are plotted in Fig. 3 for 10 different runs of five different lengths. Another indication of the statistical error is the occasional discontinuity in the curves, representing the transition between separate runs.

A more quantitative error estimate is the value of $D^*(0,r) = 1$. For 704 data points for times between 1 and $\sim 10^6$, $D^* = 1.0034 \pm 0.0049$ (mean ± SD), and $0.9879 \leq D^* \leq 1.0195$.

In the self-diffusion calculations, particles are placed randomly on the lattice at the required concentration and carry out a random walk, as described previously (Saxton, 1987b). A particle can move to any adjacent site not occupied by another particle.

The Monte Carlo calculations yield the mean-square displacement $\langle r^2 \rangle$ of an ensemble of noninteracting diffusing particles as a function of time t, and $D^*(r)$ is then found from Eq. 2. The unit of distance is the lattice spacing ℓ, and the unit of time is the reciprocal of the jump rate Γ. All diffusion coefficients D^* are normalized to one in the absence of obstacles; the normalization factor is $D(0) = \Gamma \ell^2/4$.

RESULTS

We consider the random walk of a point tracer in the presence of immobile obstacles on a triangular lattice. Obstacles are present at an area fraction c, defined as the fraction of blocked lattice sites. (This notation is often used in the lattice gas literature. In the percolation literature, the fraction of vacancies or conducting sites is p, the percolation threshold is p_c, and the fraction of blocked sites is $q = 1 - p = c$.)

To make contact with results of percolation theory, this paper treats the case of point obstacles. The effect of obstacle size is discussed briefly, but this problem will be treated in more detail in a later paper.

This section is organized as follows. First, we show plots of the mean-square displacement $\langle r^2(t) \rangle$ of diffusing particles in the presence of immobile point obstacles as a function of time, obtained from the Monte Carlo calculations. Then, we consider the range of short-range diffusion and present a scaling law for the cluster size $\langle r^2(\infty) \rangle$ at high concentrations of obstacles. Next, we define and calculate the distance-dependent diffusion coefficient $D^*(c,r)$ and the time-dependent diffusion coefficient $D^*(c,t)$. We then discuss the effect of obstacle size on the diffusion coefficient, and finally we show the distance dependence of the self-diffusion coefficient for point particles.

Values of $\langle r^2(t) \rangle$

At low concentrations of obstacles, all vacancies are connected by a continuous path and form an infinite cluster. A tracer can eventually diffuse to any vacancy, and for long times the mean-square displacement $\langle r^2(t) \rangle$ is linear in time, as shown in Fig. 1 a.

At high concentrations of obstacles, above the percolation threshold c_p, only isolated clusters of vacancies are present. Each tracer is trapped on some finite cluster, and long-range diffusion is blocked. For large t, $\langle r^2 \rangle$ approaches a finite limit $\langle r^2(\infty) \rangle$, the average size of a finite cluster, as shown in Fig. 1 b. This size depends on the concentration of obstacles and is proportional to the average radius of gyration of a cluster. The percolation threshold c_p is defined as the highest concentration of obstacles for which an infinite cluster of vacancies exists. For the triangular lattice, $c_p = \frac{1}{2}$ (Stauffer, 1985).

Scaling law for $\langle r^2(\infty) \rangle$

As shown in the Appendix, the range of diffusion above the percolation threshold can be obtained from percolation theory:

$$\langle r^2(\infty) \rangle = 0.100 \epsilon^{-2.5278}, \quad (1)$$

where $\epsilon = |c - c_p|$ is the distance from the percolation threshold. This curve, and Monte Carlo values of $\langle r^2(\infty) \rangle$, are shown in Fig. 2.

Distance- and time-dependent diffusion coefficients

We define a normalized, distance-dependent diffusion coefficient (Gaylor et al., 1979; Havlin et al., 1983) by

$$D^*(c,r) = \langle r^2(t) \rangle / t. \quad (2)$$

At low concentrations of obstacles, $\langle r^2 \rangle$ is linear in t, and the definition reduces to the usual distance-independent
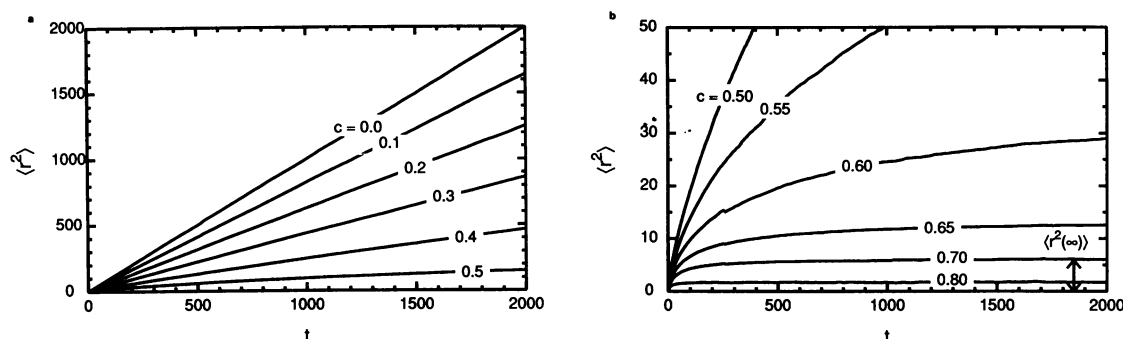
FIGURE 1 Mean-square displacement $\langle r^2 \rangle$ as a function of time t for diffusion of a point tracer on the triangular lattice in the presence of immobile point obstacles. The unit of length is the lattice constant ℓ; the unit of time is the reciprocal of the jump rate Γ. (a) Area fractions c of obstacles at and below the percolation threshold. (b) Area fractions at and above the percolation threshold. Note change in vertical scale. The value of $\langle r^2(\infty) \rangle$ for $c = 0.70$ is also shown.

diffusion coefficient $D^*(c)$. Here $D^*(c,r)$ is normalized so that $D^*(0,r) = 1$. Numerical values of $D^*(c,r)$ can be obtained directly from the Monte Carlo results shown in Fig. 1.

The physical meaning of a distance-dependent diffusion coefficient[1] is as follows. If we produce a labeled molecule at $t = 0$ and measure its diffusion over a distance r, we obtain $D^*(r)$. In a photobleaching experiment, the label is the bleached species; in a pulsed gradient spin echo NMR experiment, the precession frequency of a nuclear spin; in a diffusion-coupled chemical reaction, the chemically reactive diffusing species.

Consider an idealized picture of electron transfer by a mobile redox carrier. At $t = 0$, a source molecule transfers an electron to a carrier. The activated carrier diffuses a distance r to a sink molecule and transfers an electron to the sink. The diffusion coefficient is then $D^*(r)$. For a large number of sources and sinks in a steady state, the same picture holds, but r is the average distance between source and sink molecules. (In the experiments of Chazotte and Hackenbrock [1988], then, dilution of mitochondrial components with exogenous lipid affects the diffusion coefficient through both r and c.)

We assume ideal labeling: a label that the experimenter can see but the molecules cannot. More formally, a labeled molecule is distinguishable from an unlabeled molecule, but the presence of the label has no effect on the interaction of the labeled species with any other species in the membrane. Because the interactions are unaffected,

the molecules see no concentration gradient, and self-diffusion is measured. (The importance of the distinction between self-diffusion and concentration diffusion is discussed by Scalettar et al., 1988.)

The closest approach to an ideal label is attained in a pulsed gradient spin echo NMR measurement. In a photobleaching measurement, the ideality of the label depends on the detailed photochemistry of the bleaching process (particularly whether there is a change in the charge of the label on photobleaching).

Numerical results for $D^*(c,r)$ are shown in Fig. 3. If no obstacles are present, $D^*(0,r) = 1$ for all r, by the choice of normalization. At low concentrations of obstacles, below the percolation threshold, $D^*(c,r)$ approaches a constant value $D^*(c)$ as $r \to \infty$. This value is the asymptotic slope of the corresponding curve in Fig. 1. At high
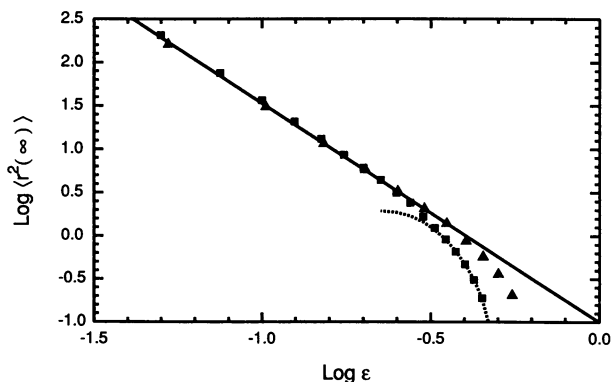

FIGURE 2 Theoretical and Monte Carlo values of $\langle r^2(\infty) \rangle$ as a function of the distance ϵ from the percolation threshold (see Appendix). (Squares), Monte Carlo results for site percolation on the triangular lattice, with $\epsilon = |c - c_p|$. (Triangles), Monte Carlo results for bond percolation on the honeycomb lattice, with $\epsilon = |b - b_c|$. (Solid line), Scaling law (Eq. 1). (Dotted line), Cluster enumeration for site percolation on the triangular lattice (Eqs. A2 and A3).

[1]Another definition of D^* was used in the preliminary version of this paper (Saxton, 1987a) and in the percolation literature (Gefen et al., 1983; Pandey et al., 1984): $D_{\ddagger}^*(c, r) = d\langle r^2(t) \rangle/dt$. At low concentrations of obstacles, the definitions are practically equivalent. At high concentrations of obstacles, $\langle r^2(t) \rangle \to \langle r^2(\infty) \rangle$, and $D_{\ddagger}^* \to 0$ faster than $D^* \sim \langle r^2(\infty) \rangle/t$ does. Eq. 2 is consistent with the physical picture of producing a label at $t = 0$ and measuring its diffusion over a distance r.
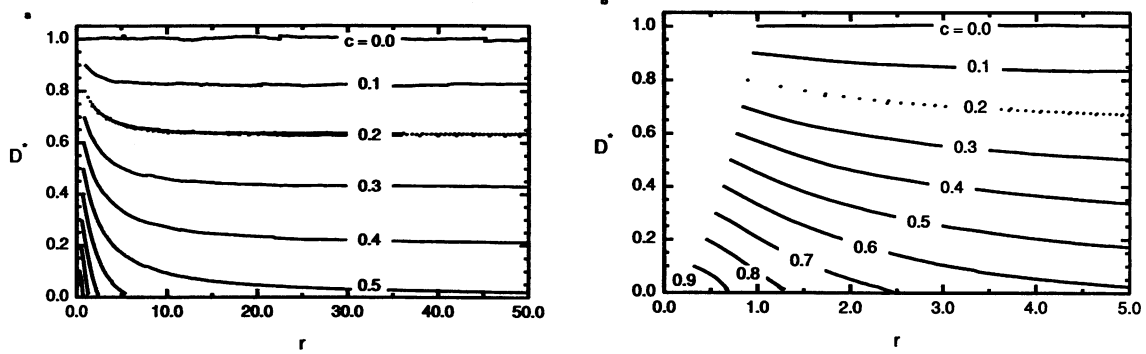
FIGURE 3 Distance dependence of the diffusion coefficient at the indicated concentrations of obstacles, for diffusion of a point tracer on the triangular lattice in the presence of immobile point obstacles. Unlabeled curves in a are identified in the expanded plot b. To show the statistical error, individual data points are shown for $c - 0.2$, for 10 different runs of five different lengths.

concentrations of obstacles, above the percolation threshold, $D^*(c,r) \rightarrow 0$ at some finite $r(\infty)$; $r(\infty)$ decreases with the concentration of obstacles, as was shown in Fig. 2. In a continuum model, the limit of D^* as $r \rightarrow 0$ would be 1 (Gaylor et al., 1979).

We can also take the data of Fig. 1 and plot D^* as a function of c with time as a parameter, as shown in Fig. 4. As t increases, D^* decreases, until the percolation threshold ($c_p = 0.50$) appears as $t \rightarrow \infty$. Part of this family of curves could be realized experimentally. If D is measured by fluorescence quenching (Blackwell et al., 1987), the time parameter in Fig. 4 corresponds to the ratio of the fluorescence lifetime of the probe to the jump time in the pure lipid. The limit $t \rightarrow \infty$ is measured in photobleaching experiments.

Effect of obstacle size

Fig. 5 shows the distance dependence of the diffusion coefficient for point tracers in the presence of immobile

point obstacles, and hexagonal obstacles of radius $R = 1$, 2, 4, 8, and 16 (Saxton, 1987b). The fraction of blocked sites is fixed at 0.3. So the total number of obstructed sites is constant, but as R increases they are grouped into fewer, larger hexagons.

As the size of the hexagons increases, the effect of the obstacles becomes smaller. The $D^*(r)$ curve falls off more slowly, because the average distance between hexagons increases, and a tracer has to diffuse farther to encounter an obstacle.

Note the strong dependence of $D^*(r)$ on obstacle size, as was found by Eisinger et al. (1986). Calculations of the concentration-dependent self-diffusion coefficient of mobile hexagons showed a much weaker dependence on R (Saxton, 1987b).

Self-diffusion

The results presented so far describe diffusion of point tracers in the presence of immobile obstacles. Similar
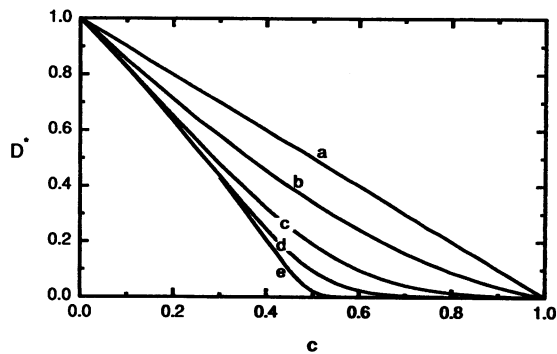

FIGURE 4 Concentration dependence of the diffusion coefficient at the indicated times for diffusion of a point tracer on the triangular lattice in the presence of immobile point obstacles. (a), $t - 1$; (b), $t - 10$; (c), $t - 10^2$; (d), $t - 10^3$; (e), $t - 10^5$.
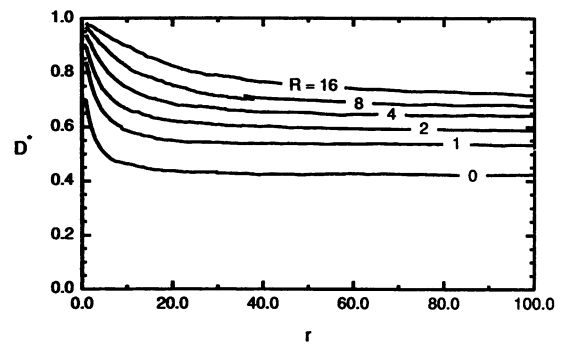

FIGURE 5 Distance dependence of the diffusion coefficient for diffusion of a point tracer on the triangular lattice in the presence of immobile point or hexagonal obstacles. The fraction of blocked points is fixed at 0.3, but they are grouped into hexagonal obstacles of radius $R - 0-16$. A 512 × 512 lattice was used in these calculations.
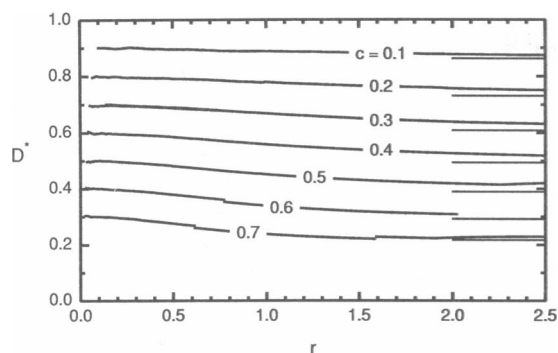
FIGURE 6 Distance dependence of the diffusion coefficient for self-diffusion of point particles on the triangular lattice at the indicated concentrations. Horizontal lines at the right show limiting values for $r \to \infty$ (Saxton, 1987b).

calculations can be carried out in which all particles are mobile, yielding the concentration-dependent, distance-dependent self-diffusion coefficient, shown in Fig. 6. Here $D^*(c,r)$ falls off very rapidly, and reaches its asymptotic value (Saxton, 1987b) within one or two lattice constants. As before, in a continuum model the value of $D^*(c,0)$ would be one. A theoretical expression for $D^*(c,r)$ shows similar behavior (Abney et al., 1989).

DISCUSSION

Biological membranes

How close are biological membranes to the percolation threshold? In those membranes for which estimates are available, the average concentration is below the percolation threshold. Estimated area fractions for several membranes are given in Table 1. These values suggest that the

TABLE 1 **Estimated area fractions of integral proteins**

Membrane	c	Reference
Red blood cell[*]	0.17	Golan et al., 1984
	0.30	Eisinger and Scarlata, 1987
Rod outer segment	0.23	Dratz and Hargrave, 1983
"Average biomembrane"	0.25	Grasberger et al., 1986
BHK cell[‡]	0.28–0.33	Quinn et al., 1984
Mitochondrial inner membrane[§]	0.4–0.5	Sowers and Hackenbrock, 1981

[*]Inside the membrane, the contribution from glycophorin is negligible. At the surface, the area occupied is significant and depends on the conformation of glycophorin.
[‡]Endoplasmic reticulum, Golgi, and plasma membrane. It is assumed that the proteins are cylinders of height 5 nm and density 1.32 g/cm^3.
[§]Calculations of c from protein concentrations and diameters are reviewed by Slater (1987).

distance dependence of D^* will not be strong. But two factors could increase the effect. First, protein distributions are not necessarily uniform; local protein concentrations could be above the percolation threshold even if the average concentration is not. Second, the estimates are for integral proteins; one must also consider the effect of peripheral proteins. If a peripheral protein is tightly bound to the membrane, it obstructs and is obstructed just as an integral protein is, so its area fraction must be included. Loosely bound peripheral proteins will act as transient obstacles; their effect is approximately the product of their area fraction and the fraction of time they are bound to the membrane. The published values for the area fraction of integral proteins are therefore lower limits on the area fraction of obstacles.

Distance scales of diffusion measurements

In Fig. 2, as the area fraction of obstacles increases, the range $\langle r^2(\infty) \rangle$ of diffusion decreases. The distance r is given in lattice constants. If we assume that each lattice point in the triangular lattice corresponds to one phospholipid, and take the lattice spacing ℓ to be 0.8 nm (Eisinger et al., 1986), we can translate Fig. 2 into physical units and find that for $c \geq 0.6$, diffusion is blocked at distances beyond ≈ 5 nm. Thus, in a photobleaching experiment (on a scale ≈ 1 μm) both the diffusion coefficient and the fractional recovery would be close to zero. But diffusion measurements by excimer formation would show a nonzero diffusion coefficient, provided that the concentration of probe was high enough that more than one probe molecule would be present in a connected region.

Distance scales are summarized in Table 2. In a diffusion measurement, the length scale may be determined by an externally imposed length, the size of the membrane, or the concentration of interacting species in a bimolecular process. Many techniques impose a time scale τ instead of a length scale, so that the corresponding length scale is $r = \sqrt{4D\tau}$ for unimolecular processes, and $r = \sqrt{8D\tau}$ for bimolecular processes.

Typical distances between molecules linked by redox carriers in mitochondria are 10–30 nm (Hackenbrock et al., 1986; Lenaz, 1988).

Comparison with experiment

The model predicts that if no obstacles are present, the diffusion coefficient is independent of distance (apart from corrections for the long-time tail in the velocity autocorrelation function, discussed in Methods). The model therefore does not account for reported differences in diffusion coefficients of pure lipids depending on the

TABLE 2 Approximate distance scales of diffusion measurements

Experiment	Length or time scale	Distance	Reference
Excimer formation	Probe concentration	1–10 nm	a
Quasielastic scattering of cold neutrons	Momentum transfer; energy resolution	2 nm	b
ESR line broadening	Probe concentration	2–8 nm	c
Electron–electron double resonance	Probe concentration	11 nm	d
Probe reorientation	Vesicle size	100–800 nm	e
Pulsed gradient spin echo NMR	Time delay between pulses	0.6–1.1 μm	f
Spot photobleaching	Radius of photobleached spot	0.5–10 μm	g
Pattern photobleaching	Period of pattern	0.5–50 μm	h

a. Eisinger et al., 1986.
b. Pfeiffer et al., 1988; Kärger et al., 1988.
c. Träuble and Sackmann, 1972; Davoust et al., 1983.
d. Feix et al., 1987.
e. Smith et al., 1981; Gawrisch et al., 1986.
f. Kärger et al., 1988.
g. Axelrod, 1985.
h. Koppel and Sheetz, 1983.

method of measurement (Kuo and Wade, 1979; Crawford et al., 1980; Feix et al., 1987; Pfeiffer et al., 1988). These differences may well be artifactual, the result of differences in sample preparation, hydration, temperature, perturbation of lipids by probe molecules, or calibration. (ESR and excimer fluorescence measurements, for example, yield a collision rate; this is converted to a diffusion coefficient by assuming a jump distance, typically taken to be 0.8 nm [Träuble and Sackmann, 1972].) If the differences in $D^*(r)$ for pure lipids were shown to be real, the explanation would require a more detailed model, allowing continuum diffusion and taking lipid structure into account.

Yechiel and Edidin (1987) measured the diffusion coefficient of NBD-phosphatidylcholine in fibroblasts by fluorescence photobleaching recovery. They found that the diffusion coefficient increased with the spot size of the laser beam, and reached a plateau at large radii. As the beam size was varied from 0.35 to 5.0 μm, D increased by a factor of 2, and the fraction of label mobile on the time scale of the experiment decreased. They attributed these results to the existence of protein-rich domains $\simeq 1$ μm in diameter.

In contrast, the model predicts that $D^*(c,r)$ decreases with r. Similar results were obtained by Gaylor et al. (1979) in their Brownian dynamics calculations of strongly interacting colloidal particles in three dimensions, and by Abney et al. (1989) in their theory of two-dimensional self-diffusion.

In the model, the probe molecule is assumed to be excluded from the obstacles. To describe these experiments, the model must be extended to allow diffusion in both regions and to include the partition coefficient of the probe between the regions. The potential importance of the partition coefficient is suggested by the observation of Yechiel and Edidin (1987) that the mobile fraction of NBD-phosphatidylcholine depends on the beam radius, but that of the lipid analogue diI-C14 does not (see also Wolf [1988]).

Eisinger et al. (1986) measured short-range lateral diffusion in erythrocytes by formation of excimers of pyrenedodecanoic acid. The minimum diffusion coefficient was 2.6 μm^2/s, and the best fit was obtained for 5.4 μm^2/s. Bloom and Webb (1983) measured long-range lateral diffusion in erythrocytes by fluorescence photobleaching recovery, and found a value of 0.82 μm^2/s for the lipid analogue diI[5] (3,3'-dioctadecylindodicarbocyanine iodide). So the observed ratio $D^*(r \rightarrow \infty)/D^*(r \rightarrow 0) = 0.15$. This ratio is not rigorously established: no common calibration standard was used in the two experiments, and the probes used were different. Note that Bloom and Webb (1983) found that the diffusion coefficient of rhodamine B phosphatidylethanolamine was about twice as large as that of diI[5].

But the model predicts a much smaller effect. For band 3 in an erythrocyte, $R = 5$ (Saxton, 1987b, Eq. 9), and $c = 0.17$–0.30 (Table 1). Calculations as in Fig. 5 give $D^*(r \rightarrow \infty)/D^*(r \rightarrow 0) = 0.66$–$0.82$. The disagreement between the model and experiment, if it is real, may well be the result of the limitations of the model: a purely hard-core interaction might not be sufficient to describe lateral diffusion. A hard-disk model of self-diffusion appears to account for about half of the observed concentration effect (Saxton, 1987b, 1988).[2] The diffusion coefficient may be affected by factors not yet included in the model, such as perturbation of lipid fluidity by proteins, and the influence of Coulomb forces and lipid-protein interactions on diffusion.

APPENDIX

Range of short-range diffusion

When the concentration of obstacles is above the percolation threshold, there is no infinite cluster, and any diffusing particle is trapped in some finite cluster of vacancies. The particle is free to diffuse in that cluster, and the range of diffusion is the size of the cluster.

The range of short-range diffusion can be obtained from percolation theory (Stauffer, 1985, section 5.2). Near the percolation threshold c_p,

$$\langle r^2(\infty) \rangle = A_0 \epsilon^{\beta - 2\nu}, \qquad (A1)$$

---

[2] In Figs. 6 b and 7 b of Saxton (1987b), the gramicidin concentrations are too high by a factor of 2. This does not affect the conclusions. I thank M. F. Blackwell for pointing out the error.

where $\epsilon = |c - c_p|$ is the distance from the percolation threshold, $\beta = 5/36$ and $\nu = 4/3$ are scaling exponents, and A_0 is a constant. (The fraction of sites belonging to the infinite cluster is $P(\epsilon) \sim \epsilon^\beta$, and the correlation length is $\xi \sim \epsilon^{-\nu}$. The radius of gyration is proportional to the correlation length, leading to the exponent 2ν in Eq. A1; the exponent β comes from averaging over cluster sizes.)

At very high concentrations of obstacles, far from the percolation threshold, $\langle r^2(\infty) \rangle$ deviates from this scaling law. But here the clusters of vacant sites are small, and we can calculate $\langle r^2(\infty) \rangle$ exactly by enumeration of clusters. We count the number $n(s,t)$ of clusters with s vacancies and t perimeter sites, and calculate the radius of gyration $r_G(s,t)$ of each cluster. If c is the probability that a site is blocked, and $1 - c$ is the probability that a site is vacant, then the probability per lattice site of finding a cluster of s vacant sites surrounded by t blocked perimeter sites is $n(s,t) (1 - c)^s c^t$. At a given concentration c of blocked sites, then, the mean-square radius of gyration is

$$\langle r_G^2(c) \rangle = \left[\sum_{st} sn(s, t)(1 - c)^s c^t r_G^2(s, t) \right] \Big/ (1 - c) \quad (A2)$$

(Feder, 1988, section 7.5; Stauffer, 1985, section 3.2). The range of diffusion is related to the mean-square radius of gyration by

$$\langle r^2(\infty) \rangle = 2\langle r_G^2(c) \rangle \quad (A3)$$

(Mitescu and Roussenq, 1983).

Thus we know the form of $\langle r^2(\infty) \rangle$ as a function of c for $c \to c_p$ and for $c \to 1$. The results are shown in Fig. 2, a log–log plot of Monte Carlo values of $\langle r^2(\infty) \rangle$ versus ϵ, and the two theoretical limits. In Eq. A1, the exponent is fixed at its theoretical value, and the constant A_0 is obtained by a least-squares fit to the Monte Carlo data, giving Eq. 1 in the text. To obtain the other theoretical limit, we use the program of Redner (1982) to enumerate clusters up to $s = 12$, and calculate $\langle r^2(\infty) \rangle$ from Eqs. A2 and A3.

Also shown in Fig. 2 are values of $\langle r^2(\infty) \rangle$ from bond percolation on the honeycomb lattice (Saxton, 1989). In bond percolation, bonds are blocked at random, and the percolation threshold b_c is defined as the highest fraction of blocked bonds for which an infinite cluster of unblocked bonds exists. Then, if b is the fraction of bonds blocked, $\epsilon = |b - b_c|$. For the honeycomb lattice, with a coordination number of 3, $b_c = 0.34729$. The close agreement of the two sets of points for small ϵ is expected from the principle of universality: critical behavior is independent of the details of lattice structure, and depends only on the dimensionality of the lattice (Stauffer, 1985).

REFERENCES

Abney, J. R., B. A. Scalettar, and J. C. Owicki. 1989. Self diffusion of interacting membrane proteins. *Biophys. J.* 55:817–833.

Axelrod, D. 1985. Fluorescence photobleaching techniques and lateral diffusion. *In* Spectroscopy and the Dynamics of Molecular Biological Systems. P. M. Bayley and R. E. Dale, editors. Academic Press, Inc., London. 163–176.

Blackwell, M. F., K. Gounaris, S. J. Zara, and J. Barber. 1987. A method for estimating lateral diffusion coefficients in membranes from steady-state fluorescence quenching studies. *Biophys. J.* 51:735–744.

Bloom, J. A., and W. W. Webb. 1983. Lipid diffusibility in the intact erythrocyte membrane. *Biophys. J.* 42:295–305.

Chazotte, B., and C. R. Hackenbrock. 1988. The multicollisional, obstructed, long-range diffusional nature of mitochondrial electron transport. *J. Biol. Chem.* 263:14359–14367.

Cowan, A. E., D. G. Myles, and D. E. Koppel. 1987. Lateral diffusion of the PH-20 protein on guinea pig sperm: evidence that barriers to diffusion maintain plasma membrane domains in mammalian sperm. *J. Cell Biol.* 104:917–923.

Crawford, M. S., B. C. Gerstein, A.-L. Kuo, and C. G. Wade. 1980. Diffusion in rigid bilayer membranes. Use of combined multiple pulse and multiple pulse gradient techniques in nuclear magnetic resonance. *J. Am. Chem. Soc.* 102:3728–3732.

Davoust, J., M. Seigneuret, P. Hervé, and P. F. Devaux. 1983. Collisions between nitrogen-14 and nitrogen-15 spin-labels. 1. Lipid-lipid interactions in model membranes. *Biochemistry.* 22:3137–3145.

Dratz, E. A., and P. A. Hargrave. 1983. The structure of rhodopsin and the rod outer segment disk membrane. *Trends Biochem. Sci.* 8:128–131.

Edidin, M. 1987. Rotational and lateral diffusion of membrane proteins and lipids: phenomena and function. *Curr. Top. Membr. Transp.* 29:91–127.

Eisinger, J., J. Flores, and W. P. Petersen. 1986. A milling crowd model for local and long-range obstructed lateral diffusion. *Biophys. J.* 49:987–1001.

Eisinger, J., and S. F. Scarlata. 1987. The lateral fluidity of erythrocyte membranes. Temperature and pressure dependence. *Biophys. Chem.* 28:273–281.

Feder, J. 1988. Fractals. Plenum Publishing Corp., New York. 283 pp.

Feix, J. B., J.-J. Yin, and J. S. Hyde. 1987. Interactions of ^{14}N:^{15}N stearic acid spin-label pairs: effects of host lipid alkyl chain length and unsaturation. *Biochemistry.* 26:3850–3855.

Galla, H.-J., W. Hartmann, U. Theilen, and E. Sackmann. 1979. On two-dimensional passive random walk in lipid bilayers and fluid pathways in biomembranes. *J. Membr. Biol.* 48:215–236.

Gawrisch, K., D. Stibenz, A. Möps, K. Arnold, W. Linss, and K.-J. Halbhuber. 1986. The rate of lateral diffusion of phospholipids in erythrocyte microvesicles. *Biochim. Biophys. Acta.* 856:443–447.

Gaylor, K. J., I. K. Snook, W. Van Megen, and R. O. Watts. 1979. Brownian dynamics studies of dilute dispersions. *Chem. Phys.* 43:233–239.

Gefen, Y., A. Aharony, and S. Alexander. 1983. Anomalous diffusion on percolating clusters. *Phys. Rev. Lett.* 50:77–80.

Golan, D. E., M. R. Alecio, W. R. Veatch, and R. R. Rando. 1984. Lateral mobility of phospholipid and cholesterol in the human erythrocyte membrane: effects of protein-lipid interactions. *Biochemistry.* 23:332–339.

Grasberger, B., A. P. Minton, C. DeLisi, and H. Metzger. 1986. Interaction between proteins localized in membranes. *Proc. Natl. Acad. Sci. USA.* 83:6258–6262.

Gut, J., C. Richter, R. J. Cherry, K. H. Winterhalter, and S. Kawato. 1982. Rotation of cytochrome P-450. II. Specific interactions of

cytochrome P-450 with NADPH-cytochrome P-450 reductase in phospholipid vesicles. *J. Biol. Chem.* 257:7030–7036.

Hackenbrock, C. R., B. Chazotte, and S. S. Gupte. 1986. The random collision model and a critical assessment of diffusion and collision in mitochondrial electron transport. *J. Bioenerg. Biomembr.* 18:331–368.

Havlin, S., D. Ben-Avraham, and H. Sompolinsky. 1983. Scaling behavior of diffusion on percolation clusters. *Phys. Rev. A.* 27:1730–1733.

Hui, S.-W. 1987. Ultrastructural studies of the molecular assembly in biomembranes: diversity and similarity. *Curr. Top. Membr. Transp.* 29:29–70.

Jacobson, K., A. Ishihara, and R. Inman. 1987. Lateral diffusion of proteins in membranes. *Annu. Rev. Physiol.* 49:163–175.

Kärger, J., H. Pfeifer, and W. Heink. 1988. Principles and application of self-diffusion measurements by nuclear magnetic resonance. *Adv. Magn. Reson.* 12:1–89.

Kleinfeld, A. M. 1987. Current views of membrane structure. *Curr. Top. Membr. Transp.* 29:1–27.

Koppel, D. E., and M. P. Sheetz. 1983. A localized pattern photobleaching method for the concurrent analysis of rapid and slow diffusion processes. *Biophys. J.* 43:175–181.

Kuo, A.-L., and C. G. Wade. 1979. Lipid lateral diffusion by pulsed nuclear magnetic resonance. *Biochemistry.* 18:2300–2308.

Lenaz, G. 1988. Role of mobility of redox components in the inner mitochondrial membrane. *J. Membr. Biol.* 104:193–209.

Lenaz, G., and R. Fato. 1986. Is ubiquinone diffusion rate-limiting for electron transfer? *J. Bioenerg. Biomembr.* 18:369–401.

McCloskey, M., and M.-M. Poo. 1984. Protein diffusion in cell membranes: some biological implications. *Int. Rev. Cytol.* 87:19–81.

Millner, P. A., and J. Barber. 1984. Plastoquinone as a mobile redox carrier in the photosynthetic membrane. *FEBS (Fed. Eur. Biochem. Soc.) Lett.* 169:1–6.

Mitescu, C. D., and J. Roussenq. 1983. Diffusion on percolation clusters. *Ann. Isr. Phys. Soc.* 5:81–100.

Pandey, R. B., D. Stauffer, A. Margolina, and J. G. Zabolitzky. 1984. Diffusion on random systems above, below, and at their percolation threshold in two and three dimensions. *J. Stat. Phys.* 34:427–450.

Peters, R. 1985. Lateral mobility of proteins in membranes. *In* Structure and Properties of Cell Membranes. Vol. I. G. Benga, editor. CRC Press, Boca Raton, FL. 35–50.

Pfeiffer, W., G. Schlossbauer, W. Knoll, B. Farago, A. Steyer, and E. Sackmann. 1988. Ultracold neutron scattering study of local lipid mobility in bilayer membranes. *J. Phys. (Paris).* 49:1077–1082.

Pusey, P. N., and R. J. A. Tough. 1985. Particle interactions. *In* Dynamic Light Scattering: Applications of Photon Correlation Spectroscopy. R. Pecora, editor. Plenum Publishing Corp., New York. 85–179.

Quinn, P., G. Griffiths, and G. Warren. 1984. Density of newly synthesized plasma membrane proteins in intracellular membranes II. Biochemical studies. *J. Cell Biol.* 98:2142–2147.

Redner, S. 1982. A FORTRAN program for cluster enumeration. *J. Stat. Phys.* 29:309–315.

Saxton, M. J. 1987a. Lateral diffusion in an archipelago: the distance dependence of the diffusion constant. *Biophys. J.* 51:542a. (Abstr.)

Saxton, M. J. 1987b. Lateral diffusion in an archipelago: the effect of mobile obstacles. *Biophys. J.* 52:989–997.

Saxton, M. J. 1988. Lateral diffusion in an archipelago: the effect of large mobile obstacles. *Biophys. J.* 53:510a. (Abstr.)

Saxton, M. J. 1989. The spectrin network as a barrier to lateral diffusion in erythrocytes: a percolation analysis. *Biophys. J.* 55:21–28.

Scalettar, B. A., J. R. Abney, and J. C. Owicki. 1988. Theoretical comparison of the self diffusion and mutual diffusion of interacting membrane proteins. *Proc. Natl. Acad. Sci. USA.* 85:6726–6730.

Slater, E. C. 1987. The mechanism of the conservation of energy of biological oxidations. *Eur. J. Biochem.* 166:489–504.

Smith, L. M., H. M. McConnell, B. A. Smith, and J. W. Parce. 1981. Pattern photobleaching of fluorescent lipid vesicles using polarized laser light. *Biophys. J.* 33:139–146.

Sowers, A. E., and C. R. Hackenbrock. 1981. Rate of lateral diffusion of intramembrane particles: measurement by electrophoretic displacement and rerandomization. *Proc. Natl. Acad. Sci. USA.* 78:6246–6250.

Stauffer, D., 1985. Introduction to Percolation Theory. Taylor & Francis, London. 124 pp.

Träuble, H., and E. Sackmann. 1972. Studies of the crystalline-liquid crystalline phase transition of lipid model membranes. III. Structure of a steroid-lecithin system below and above the lipid-phase transition. *J. Am. Chem. Soc.* 94:4499–4510.

Wolf, D. E. 1988. Probing the lateral organization and dynamics of membranes. *In* Spectroscopic Membrane Probes. Vol. I. L. M. Loew, editor. CRC Press, Boca Raton, FL. 193–220.

Yechiel, E., and M. Edidin. 1987. Micrometer-scale domains in fibroblast plasma membranes. *J. Cell Biol.* 105:755–760.